

Self-consistent GW and higher-order calculations of electron states in metals

Eric L. Shirley

National Institute of Standards and Technology, Optical Technology Division, Gaithersburg, Maryland 20899

(Received 6 June 1996)

Past work, treating simple metals in the GW approximation, has largely neglected effects of self-consistency and higher-order vertex corrections on occupied bandwidths. This work presents self-consistent GW results, plus nearly self-consistent higher-order results, for jellium, illustrating that both effects are large, yet largely canceling (e.g., 0.65-eV effects on the sodium bandwidth, but a combined effect of only 0.13 eV). This supports findings that many-body effects substantially reduce such bandwidths. [S0163-1829(96)01736-5]

INTRODUCTION

The notion of electron energy bands continues to provide fundamental insight into understanding basic properties of solids. Lately, the newfound capacity for *ab initio* prediction of band energies has stimulated materials research all the more. Such an accomplishment relies on the abilities both to solve the one-electron Schrödinger equation in a crystal, and to determine many-body corrections to electron band energies, i.e., to determine self-energy effects. The role of self-energy effects is particularly clear when computing band gaps in insulating systems: e.g., the standard local-density approximation (LDA) (Ref. 1) predicts a band gap of 0.55 eV for silicon vs the measured value 1.17 eV, whereas inclusion of self-energy effects leads to a gap around 1.29 eV.² Equally fundamental quantities are the occupied bandwidths in simple metals, quantities perhaps considered first in the classic Sommerfeld theory, which the LDA may overestimate by about 10%.³

Currently, the most successful approach which describes electron excitations in solids uses diagrammatic techniques to estimate self-energy effects. The electron Green's function G obeys Dyson's equation⁴

$$[E + \frac{1}{2} \nabla_{\mathbf{r}}^2 - V_{\text{ext}}(\mathbf{r}) - V_H(\mathbf{r})]G(\mathbf{r}, \mathbf{r}'; E) - \int d^3\mathbf{r}'' \Sigma(\mathbf{r}, \mathbf{r}''; E)G(\mathbf{r}'', \mathbf{r}'; E) = 0. \quad (1)$$

Σ is the self-energy operator. V_{ext} and V_H are external and Hartree potentials. The exact G and Σ may be found using well-known coupled equations⁵

$$G(12) = G_0(12) + \int d(34)G_0(13)\Sigma(34)G(42),$$

$$\Sigma(12) = i \int d(34)G(13^+)W(14)\Gamma(34, 2),$$

$$W(12) = \nu(12)$$

$$+ \int d(3456)\nu(13)\Gamma(45, 3)G(46)G(65)W(62),$$

$$\Gamma(12, 3) = \delta(12)\delta(13)$$

$$+ \int d(4567)\Gamma(67, 3)G(46)G(75)\frac{\delta\Sigma(12)}{\delta G(45)}. \quad (2)$$

G_0 is the Green's function when $\Sigma = 0$, ν the bare electron-electron interaction, and W the dynamically screened interaction. The above arrangement of equations facilitates expansion of Σ using W , not ν , avoiding divergences associated with ν . Hopefully, this expansion also converges rapidly as terms with increasing powers of W are included, because of W 's smallness. In practice, the coupled expansions of G , Σ , W , and Γ must be terminated at some level. Beyond Hartree's approximation ($\Sigma = 0$), one next assumes $\Gamma = \delta(12)\delta(13)$, producing $\Sigma(12) \approx iG(12^+)W(21)$.

For many materials this "GW approximation" has yielded remarkably accurate, predicted band energies,^{2,6} but two significant caveats remain largely unaddressed. In principle, expansion of Σ should be carried out using the self-consistent, renormalized G . In practice, though, only an unrenormalized G has been used. Depending on the solid, from 10% to 50% of spectral weight in G is transferred from quasiparticle peaks by self-energy effects, to form plasmons and other satellites, the "incoherent" part of G . Also, little work has quantitatively assessed the role of *dynamical* vertex corrections (higher terms in Γ), in studies of realistic systems. One can speculate that simultaneous neglect of renormalization and vertex corrections produces two, largely canceling errors in the behavior of Σ : e.g., one can obtain a density-response function which obeys the f -sum rule, when both effects are omitted or included, whereas inclusion of one effect without the other can have drastic consequences regarding adherence to that rule.⁷

Simple metals have provided a great challenge for spectroscopic measurement of electron excitations,⁸ and assessment of the role of vertex corrections when describing such excitations.^{3,9} Here I present fully self-consistent GW calculations, which use a renormalized G , for jellium with Wigner-Seitz radius r_s ranging from 2 to 5, and nearly self-consistent calculations at the same densities, which include lowest-order *dynamical* vertex corrections. Compared to one-electron theory, a self-consistent GW treatment produces no substantial reduction in the occupied bandwidth

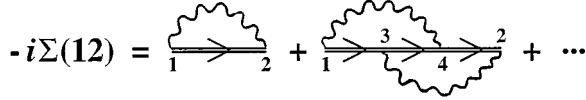


FIG. 1. Low-order diagrams for electron self-energy (Σ), in terms of renormalized Green's function G (double line) and dynamically screened interaction W (wavy line).

(henceforth simply “bandwidth”), as does a GW treatment with an unrenormalized G , but rather an increase. Including vertex corrections restores a reduction in bandwidth, and the results suggest that effects of any remaining non-self-consistency (in the higher-order calculations) are minor. Thus, renormalization of G and vertex corrections can each have significant effects, but the combined effects largely cancel. In what follows, I elaborate further on technical details, present the main results, and discuss the comparison of this and other work. I also suggest directions for future theoretical and experimental work, and provide some conclusions.

COMPUTATIONAL DETAILS

Given an adequate expression for W , evaluating G is reduced to expanding Σ using G , which remains to be solved self-consistently, and W . This yields (see Fig. 1)

$$\begin{aligned} -i\Sigma(12) &= G(12^+)W(21) \\ &+ i \int d(34)G(13)W(14)G(34)W(32)G(42) \\ &+ \dots \end{aligned} \quad (3)$$

This work terminates Σ after two terms, a nonconserving approximation,⁷ but the magnitude of related problems should vary only as higher-order effects. W is $\epsilon^{-1}\nu$, where ϵ is the dielectric function. For densities considered, a plasmon-pole model for ϵ^{-1} suffices.³ The model used here gives accurate ω and ω^{-1} moments of $\text{Im}\epsilon^{-1}(q, \omega)$, as dictated by the f -sum rule and (through Kramers-Krönig relations) by $\text{Re}\epsilon^{-1}(q, \omega=0)$, which is found using

$$\epsilon(q, \omega=0) = 1 - \nu(q) \frac{\chi^0(q, \omega=0)}{1 - f(q)\chi^0(q, \omega=0)}, \quad (4)$$

where $\chi^0(q, \omega)$ is the Lindhard polarizability, and $f(q)$ facilitates a good fit, at all r_s considered, to quantum Monte Carlo data for $\epsilon^{-1}(q, \omega=0)$:¹⁰

$$f(q) = K_{xc}(n) [k_F^2 / (k_F^2 + 0.08q^2)]. \quad (5)$$

$K_{xc}(n)$ is $dV_{xc}(n)/dn$, and $V_{xc}(n)$ is the exchange-correlation potential¹ in an electron gas with density n and Fermi momentum k_F .

There is less known about G *a priori*, although Ceperley-Alder electron-gas data¹¹ provide two absolute criteria for validity of a given G . For Fermi energy E_F , one knows $E_F = k_F^2/2 + V_{xc}(n)$, and $V_{xc}(n)$ may be found at all densities from the data. Also, the total energy per electron (E/N) should agree with that found using the Galitskii-Migdal formula,¹²

$$\frac{E}{N} = \frac{\int d^3k \int_{-\infty}^{E_F} dE A(\mathbf{k}, E) \frac{1}{2} (E + k^2/2)}{\int d^3k \int_{-\infty}^{E_F} dE A(\mathbf{k}, E)}. \quad (6)$$

$A(\mathbf{k}, E)$ is the spectral function $A(\mathbf{k}, E) = |\text{Im} G(\mathbf{k}, E)|/\pi$.

In the GW approximation, working within a plasmon-pole model, one may write

$$\begin{aligned} \Sigma(\mathbf{k}, E) &= +i \int \frac{d^3q}{(2\pi)^3} \nu(q) \int \frac{d\omega}{2\pi} e^{+i\eta\omega} \\ &\times \left[\int_{-\infty}^{E_F} d\epsilon \frac{A(\mathbf{k}+\mathbf{q}, \epsilon)}{E + \omega - \epsilon - i\eta} + \int_{E_F}^{\infty} d\epsilon \frac{A(\mathbf{k}+\mathbf{q}, \epsilon)}{E + \omega - \epsilon + i\eta} \right] \\ &\times \left[1 + \frac{\omega_p^2}{2\omega_q} \left(\frac{1}{\omega - \omega_q + i\eta} - \frac{1}{\omega + \omega_q - i\eta} \right) \right], \end{aligned} \quad (7)$$

with η being a positive infinitesimal, and ω_p and ω_q being plasma and plasmon-pole frequencies, respectively. Σ has a real, energy-independent term, because of the constant in the second bracketed factor, plus two energy-dependent terms. The imaginary part of the first (second) term is the frequency convolution of the advanced (retarded) spectral function for G and retarded (advanced) “spectral function” for W .

When evaluating $G(\mathbf{k}, E)$ from $G_0(\mathbf{k}, E)$ and $\Sigma(\mathbf{k}, E)$, the energy dependence of $\text{Re}\Sigma(\mathbf{k}, E)$ reduces quasiparticle pole strengths, as the spectral weight shifts to energies where $\text{Im}\Sigma(\mathbf{k}, E)$ is nonzero, primarily further than ω_p from E_F , below and above E_F . Effects of renormalizing G , when a given G is used to compute Σ , include quasiparticle pole strengths being closer to unity, and the correlation-induced bandwidth reduction being weakened. This correlation-induced reduction competes with a comparable exchange-induced increase (because of the energy-independent term in Σ), so a 10% change in bandwidth is a rather delicate effect.

Regarding the sensitivity of a computed Σ to the input G , renormalization is more important than mere bandwidth compression (where quasiparticles retain unity pole strength), provided that the input E_F is approximately right, which can usually be achieved by rigidly shifting the energy of all spectral weight as needed. To illustrate this, many-body effects reduce the sodium ($r_s = 3.96$) bandwidth by ≈ 0.6 eV, while we have $\hbar\omega_p \approx 6$ eV. So renormalizing G shifts the spectral weight (with respect to E_F) by about 6 eV (plus or minus some of the 2.65-eV bandwidth), while bandwidth narrowing correspondingly shifts spectral weight by tenths of an eV.

I first performed “nonrenormalized” (using a G_0 shifted to have the correct E_F) and “renormalized” (using a self-consistent G) GW calculations, by tabulating $A(\mathbf{k}, E)$ [$\equiv A(|\mathbf{k}|, E)$] on an energy-momentum grid (4000 E 's, at intervals ranging from 0.005 to 0.001 a.u., and 600 $|\mathbf{k}|$'s, at intervals ranging from 0.006 to 0.010 a.u., interval sizes varying with r_s). Slightly coarser grids produced similar results; (small) effects of electron states at all higher momenta or energies were estimated and included. In essence, the above equation and Dyson's equation were solved self-consistently. Care was taken to describe both discrete poles

TABLE I. For various r_s , renormalization constants (Z 's) at $k=0$ and $k=k_F$, occupied bandwidth w (eV), and E_F (hartree). Results are given for nonrenormalized (fully self-consistent) GW approaches and for a higher-order approach, and exact values for E_F are given.

r_s	GW			Higher order			Exact
	$Z(0), Z(k_F)$	w	E_F	$Z(0), Z(k_F)$	w	E_F	E_F
2	0.59,0.77 (0.63,0.81)	11.89 (13.28)	0.100 (0.130)	0.53,0.75	11.57(5)	0.081	0.103
3	0.52,0.69 (0.58,0.74)	5.03 (5.95)	-0.052 (-0.036)	0.48,0.67	5.04(4)	-0.060	-0.042
4	0.47,0.63 (0.55,0.70)	2.63 (3.28)	-0.091 (-0.083)	0.45,0.61	2.66(4)	-0.091	-0.075
5	0.43,0.58 (0.53,0.66)	1.59 (2.28)	-0.099 (-0.083)	0.39,0.56	1.72(4)	-0.093	-0.082

and continua in $A(\mathbf{k}, E)$ adequately. Evaluating $\text{Re}\Sigma$ included the Kramers-Krönig transformation of $\text{Im}\Sigma$. This was done only after convoluting $\text{Im}\Sigma$ with a (0.016 hartree)-full-width tepee function: otherwise, spurious gaps in continuous parts of $\text{Im}\Sigma$ (because of discrete integration over q) induced spurious oscillations in $\text{Re}\Sigma$.

I next used resulting spectral functions as input to higher-order (vertex-corrected) calculations of Σ . Then, though, only quasiparticle properties were examined: incoherent parts of G were not studied further. For each \mathbf{k} , this permitted approximating occupied and unoccupied, incoherent parts of G each as one pole to three poles, while the coherent part had one pole. Σ was found using analytical frequency, and Monte Carlo momentum integrations. The balance of $1/q^2$ Coulomb-potential and q^2 phase-space factors (associated with interaction-line momentum integrations) provided importance sampling. Results were converged with respect to the maximum q sampled, and care was taken with regard to spurious fluctuations in $\text{Re}\Sigma$ because of the higher-order term. (Such fluctuations resulted from imperfect sampling: there was quasiparticle decay because of interaction with the electron-hole continuum. Whereas these interactions are suppressed at the GW level, provided one uses a plasmon-pole model, these interactions are only partially suppressed at the next-higher-order level, even when using a plasmon-pole model.)

Bandwidths and quasiparticle pole strengths in higher-order results were found in two ways: (A) a G_0 , shifted to correct E_F , was used to compute Σ in GW , and the resulting, non-self-consistent (renormalized) spectral function was used as input for a higher-order calculation; or (B) the self-consistent GW spectral function was used as that input. In comparing methods (A) and (B), method (A) produced closer consistency in bandwidths and pole strengths input and output by the higher-order calculation, so results (A) are presented. Insensitivity of final results to such distinctions of input G 's suggest that these higher-order results exhibit minimal residual, non-self-consistency effects.

I shifted spectral weights in G 's rigidly to achieve the correct E_F , when preparing input for all self-energy calculations, except in iterations beyond the first in the self-consistent calculations. This prevented complete self-consistency for E_F , but permitted a more absolute investigation of the role of various diagrams in Σ . Achieving

the correct E_F also permitted an association of accuracy in the total energy (computed *à la* Galitskii-Migdal) with accuracy in the degrees of normalization and bandwidth reduction. Computed total energies were affected far more by renormalization than by bandwidth reduction, and were too positive when obtained from the Galitskii-Migdal formula using an unrenormalized G .

RESULTS

Tables I and II show nonrenormalized and self-consistent GW results, and higher-order results for computed bandwidths, quasiparticle pole strengths, E_F 's, and total energies, plus known values of the last two quantities. The total energies obtained by Lundqvist are also given,¹³ as are the total energies obtained by Hartree-Fock. Figure 2 shows spectral functions (for $r_s=4$) used as input to higher-order calculation in approaches (A) and (B).

Jellium and simple metals Al, Li, Na, and K have been treated at a nonrenormalized but otherwise self-consistent GW level by Northrup, Surh, Hybertsen, and Louie (NSHL).³ These metals have nominal r_s 's of 2.07, 3.25, 3.96, and 5.86, respectively, but their one-electron bandwidths and many-body bandwidth corrections differ somewhat from corresponding jellium results. To estimate what a

TABLE II. For various r_s , total energy per electron, E/N (hartrees). Results for the present nonrenormalized (fully self-consistent) GW approaches, those given in Ref. 13, and exact values. Based on results of the higher-order calculations (in text), lesser weight should be given to the present, self-consistent GW results.

r_s	E/N			
	Present GW	Ref. 13	Hartree-Fock	Exact
2	-0.004 (-0.003)	-0.005	0.047	0.002
3	-0.070 (-0.068)	-0.069	-0.030	-0.067
4	-0.078 (-0.073)	-0.078	-0.045	-0.077
5	-0.074 (-0.073)	-0.076	-0.047	-0.076

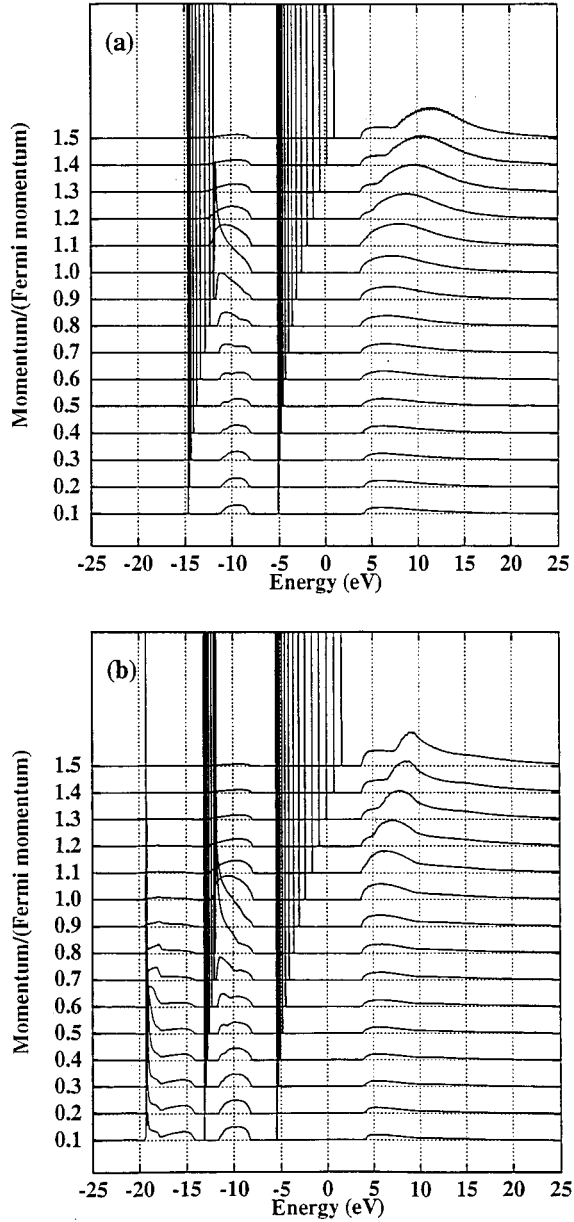


FIG. 2. Partially renormalized (a) and fully renormalized (*à la* GW) (b) electron spectral functions for $r_s = 4$. The spectral function is plotted in arbitrary units, in stack-plot fashion, for various momenta and energies, and discrete poles are indicated by spikes. For a given momentum, the base line is chosen so that a value of zero for the spectral function corresponds to the indicated momentum on the left-hand axis. Furthermore, whereas all results here have been normalized similarly for the sake of presentation, the integral of each spectral function over all energy is unity.

higher-order, renormalized, self-consistent treatment would give for bandwidths in these metals, I adjust NSHL's jellium corrections by combining (1) discrepancies between my jellium results and their jellium GW results with (2) their computed discrepancies between many-body corrections in jellium and the real materials. This gives respective bandwidths of 10.2(1) eV, 3.08(8) eV, 2.68(5) eV, and 1.86(11) eV.¹⁴ There are only small differences from NSHL's accurate results. Available experimental bandwidths are 10.6(1) eV for

Al, 2.65(5) eV for Na, and 1.60(5) eV for K. Considering separate effects of renormalization or vertex corrections, the final agreement with experiment is no worse than warranted, differences being much smaller than the changes produced when either effect is taken separately.

DISCUSSION

Besides differences in bandwidths and renormalization constants, there are further differences between the results of Figs. 2(a) and (b). There are more features in Fig. 2(b) than in Fig. 2(a). Meanwhile, the satellites present in both parts differ somewhat. Before discussing the results both above and below the occupied quasiparticle band, a few points should be mentioned. First, what are discrete poles in these figures, when using a plasmon-pole model, should broaden somewhat when such a model is abandoned. This is because of quasiparticle damping which would occur because of interactions with the electron-hole continuum, except for states at energy E_F . Second, satellites are easily motivated as resulting from the frequency convolution implicit in Eq. (7). Where the self-energy has a nonzero imaginary part, there is nonzero spectral weight. Features present only in Fig. 2(b) are motivated as resulting from the frequency convolution in Eq. (7) of satellites built into the renormalized spectral function in Eq. (7). All such higher-order features should be viewed with particular scrutiny here, however, because inclusion of vertex corrections is required to form a complete picture of these features and other, equally important effects.

Describing satellites is simplest above E_F . There, spectral weight is confined to lie at energies above $E_F + \hbar\omega_p$: this is the onset of the quasihole-plasmon continuum in a system where electrons would not couple to plasmons, but the coupling (in the interacting case) introduces nonzero one-electron spectral weight in this energy region. Meanwhile, there is a particularly large density of states around $\hbar\omega_p$ plus the quasiparticle energy, which may be attributed to the fact that the partial plasmon density of states, weighted in the self-energy, has a maximum at $\hbar\omega_p$, and is strictly zero below that energy. Additional structure may be seen in Fig. 2(b) around $2\hbar\omega_p$ plus the quasiparticle energy, which (presumably) is a satellite of the peak around $\hbar\omega_p$ plus the quasiparticle energy.

Below the occupied quasiparticle band, the spectral weight is confined to lie at energies below $E_F - \hbar\omega_p$, the onset of the quasihole-plasmon continuum. (The reader is reminded that, below E_F , energies of many-body states created when *removing* an electron *increase* to the left.) A discrete pole is sometimes present to the left of a broad feature at low momenta. In Fig. 2(b), satellites themselves gives rise to further satellites, so that even third-order effects are barely discernible at sufficiently low energy and momentum. The origin of discrete poles in satellites is motivated in detail in the Appendix. The limited energy range spanned by features below the occupied band, as opposed to by those above that band, is easily motivated: the occupied spectral weight lies within a more compact part of the energy-momentum phase space. However, the rule

$$\int_{-\infty}^{\infty} d\omega A(k, \omega) = 1 \quad (8)$$

still limits the overall filling of the phase space by the spectral weight function.

In comparison to other work, the GW results agree well with those of Lundqvist,¹⁵⁻¹⁷ who performed extensive GW calculations using one iteration of Dyson's equation, and at least some calculations with two or more iterations, although the nature of the Green's-function input into the self-energy on the second iteration is not clear to the present author. In some work, Lundqvist also used a different plasmon-pole model than that used here.¹⁶ Indeed, it was a model whose static dielectric function differed from that given by a random-phase-approximation (RPA) treatment in a fashion opposite to the way that the present, static dielectric function differs. Lundqvist also carried out analogous results using the full, RPA dielectric function (i.e., no plasmon-pole model was used).¹⁷ The results were quite similar to those using Lundqvist's plasmon-pole model, and Lundqvist's total-energy results¹³ are based on a full, RPA treatment (and the Galitskii-Migdal formula). Also, Lundqvist discussed, in less detail, the additional discrete poles treated in the Appendix.

Hedin has also considered the $GWGWG$ term, in conjunction with several additional approximations.¹⁸ Furthermore, his work (and references therein) touch on many issues related to those discussed here. As for other theoretical aspects discussed in that work, issues regarding appropriateness of expansions of the Green's function and self-energy to various orders of W are raised. As cited by Hedin, it has been argued¹⁹ that expansion of G , rather than of the self-energy, should be performed consistently at each order. In these regards, the higher-order results in this work omit contributions to G which are, at lowest, third order in W . Again, the argument for the smallness of such terms may be invoked, although a better understanding of the difficulties which might occur in self-energy calculations may be a worthwhile basis for further work. Hedin also presents three sum rules for the spectral function, which are followed automatically throughout the present work, at least at the GW level. (One subtlety, however, is that, when evaluating the first frequency moment of the spectral function, care must be taken to evaluate the Fock term in the self-energy using the renormalized G , which reflects single-particle occupancies differing from the occupancies found in a noninteracting picture.) Meanwhile, further care may be needed in this work to fully analyze satellites output by the higher-order calculations.

Interestingly, Hedin provides results for the oscillator strengths of the first plasmon satellites for $r_s=2$. It is difficult to compare these results with those presented here, directly, but an attempt shall now be made. Difficulties in comparison arise because (1) the results by Hedin ostensibly reflect a different set of approximations than those made here, (2) issues regarding the degree of self-consistency achieved in Hedin's work are not clear, (3) certain details depend on one's assumed dielectric function, and (4) there is ambiguity regarding the precise corresponding quantity in the present results. Therefore, I instead consider the total occupied incoherent spectral weight output by the non-self-consistent GW calculations, which should be close to the analogous results of the (nearly self-consistent) higher-order calculations. This substitute should bias positively my estimate of the *relative oscillator strength* of the first plasmon

peak (relative to that of the quasiparticle peak), especially at the bottom of the band. Indeed, my relative strength is 0.66, compared to 0.54 found by Hedin, at the bottom of the band, coinciding with Hedin's results for $k \approx k_F/2$, and being 0.08 at the Fermi momentum, compared to Hedin's 0.21. Thus, this level of agreement is satisfactory.

The Γ used in Refs. 9 and 20, henceforth called Γ' , in replacing $\Sigma \approx iGW \rightarrow \Sigma \approx iGW\Gamma'$, might not represent the true Γ . It is readily shown that, when used with a renormalized G , the true Γ must depend on *two* momentum-frequency combinations—not only that of an interaction line—to satisfy the f -sum rule. However, Γ' has only the later dependence. Indeed, Ref. 9 finds effects of the above replacement opposite to those found here. At least one work²¹ examines the higher-order correction used here, for silicon, but using an unrenormalized G , finding minor effects for vertex corrections in silicon, in agreement with others.^{2,20} Such authors²¹ are presumably the first to consider the higher-order corrections in a more complete model than jellium.

Incoherent parts of electron spectral functions have enjoyed relatively little, unambiguous experimental manifestation, partly because their signals are frequently superposed with those of lifetime-broadened coherent parts in photoemission or x-ray emission spectra, or with secondary-electron background. Resonant x-ray fluorescence experiments, made practical by third-generation light sources,²² might reveal occupied incoherent parts more clearly. In principle, they could isolate fluorescence by occupied plasmons just outside of the Fermi sea in alkali metals, where the coherent parts should not exhibit fluorescence. Core holes could be created at such momenta using resonant photoexcitation to just above E_F . In particular, the proposed experiment may provide tremendous momentum selectivity, the desirability of which was noted by Hedin.¹⁸ However, spectra may also reveal phonon- and plasmon-assisted self-energy effects and/or nonvertical recombinations with quasiparticles in the Fermi sea, or x-ray-edge effects.²³

One potential, future extension of this work would be to cease using a plasmon-pole ansatz. However, it is not trivial to go about this, since the frequency dependence of the true dielectric function is not as well known as its static value. This work was carried out to maximize accuracy in the latter. Nonetheless, because such an ansatz may affect bandwidth compression by many-body effects by only 25%,²⁴ whereas the effects of self-consistency and the $GWGWG$ term can affect that compression by 200%, the conclusions of this work should be unaffected by use of a plasmon-pole model. More fundamentally, this work should apply primarily to simple metals and conventional semiconductors. [In the latter, the smallness of band gaps (vs bandwidths and plasma frequencies) and the nearly-free-electron character of valence and conduction bands permit one to entertain that assertion.]

On the other hand, the approach of GW or higher-order self-energy calculations to more strongly correlated systems presents a greater challenge. GW calculations have been carried out with great success in Ni,²⁵ but to a lesser degree of success in NiO.²⁶ This suggests a more complex nature of correlation in transition-metal oxides and other similar compounds, as corroborated by the quantum Monte Carlo results of Mitás,²⁷ who found that the correlation energy in MnO was more difficult to account for than in other systems, such

as silicon. Obviously, the strong correlation in many systems indicates the greater difficulty in finding a diagrammatic expansion to describe correlation effects. Of interest in their own right, strongly correlated systems are beyond the scope of this work.

Finally, consider the range of densities examined, which represents typical metallic systems. At densities higher than those considered, the bandwidth exceeds $\hbar\omega_p$, leading to unreliability of a plasmon-pole model,³ whereas the correlation effects should still be well treated by a full *GW* treatment. At densities lower than those considered, correlations should become increasingly stronger with increasing r_s , so that the convergence of an expansion such as the one used here must eventually become doubtful. For instance, one may consider the breakdown of a jellium picture noted in Ref. 10, and references therein.

CONCLUSIONS

In summary, I examined effects of self-consistency (detailed renormalization) and *dynamical* vertex corrections on predicted properties of metals. While a non-self-consistent, low-order (*GW*) treatment reduces occupied bandwidths by 10–30 % (compared to independent-electron theory), self-consistency leads to overall increased bandwidths. Subsequent inclusion of the next-order term in $\Sigma(GWG WG)$ restores reduced bandwidths, which agree well with experiment. The *GWGWG* term was typically a tenth as large as the *GW* term, suggesting that even higher-order terms are correspondingly smaller, affecting bandwidths minimally.

In many solids, bandwidths and plasmon energies are larger than crystal-potential effects on energy bands. Hence, these results may describe effects in many solids characterized reasonably as nearly-free-electron systems, ranging from simple metals to conventional semiconductors. However, future investigations should address both ramifications of going beyond a plasmon-pole model in such systems, as well as consider tackling the many-body physics present in more strongly correlated systems, such as transition-metal oxides.

ACKNOWLEDGMENTS

I profited from discussions with D. R. Penn, Z. H. Levine, M. D. Stiles, M. P. Surh, and R. U. Datla.

APPENDIX

Here the presence of discrete poles in the incoherent, occupied spectral weight in Fig. 2(a) is motivated. Other discrete poles may occur for analogous reasons. This motivation uses an intuitive picture based on a model Hamiltonian. Consider states involving either one hole, or one hole and one plasmon. Conservation of momentum permits us to consider only one state having a hole, labeled $|q\rangle$, and the subset of hole-plus-plasmon states having the same total momentum, $\{|p\rangle\}$. In the basis of all states mentioned, the Hamiltonian would be diagonal, except that $|q\rangle$ is coupled to each state, $\{|p\rangle\}$, with coupling V_{pq} . One has, therefore, such a Hamiltonian:

$$\hat{H} = \epsilon_q^0 |q\rangle\langle q| + \sum_p [\zeta_p^0 |p\rangle\langle p| + (V_{pq} |p\rangle\langle q| + \text{H.c.})].$$

We desire the partial density of states (PDOS)

$$S(E) = \frac{1}{\pi} \left| \text{Im} \left\langle q \left| \frac{1}{E + i\eta - \hat{H}} \right| q \right\rangle \right|.$$

Meanwhile, the reader is reminded that, because we are discussing hole states, higher-energy solutions of this Hamiltonian are reflected at lower energies in the electron spectral function.

The energies ϵ_q^0 and ζ_p^0 are those of *noninteracting* hole or hole-plus-plasmon states. Only at the former would the above PDOS be nonzero, in the absence of any coupling. In the present of coupling, some of the PDOS is transferred to the range (R) spanned by $\{\zeta_p^0\}$, and the pole, originally at ϵ_q^0 , will move because of level-repulsion effects. This can all be demonstrated using first- and second-order Rayleigh-Schrödinger perturbation theory. However, in certain circumstances, a discrete pole also forms at even higher energies, provided that R is limited.

The exact PDOS may be found analytically, being given as

$$S(E) = \frac{1}{\pi} \left| \text{Im} \left(\frac{1}{E + i\eta - \epsilon_q^0 - \sum_p |V_{pq}|^2 / (E + i\eta - \zeta_p^0)} \right) \right|.$$

By inspection, one can already infer a nonzero PDOS at a pole lower than ϵ_q^0 , as well as spectral weight occurring when E lies within R . Meanwhile, the real part of the denominator will be zero for at least two energies, once at the pole already mentioned, and once elsewhere. To estimate both energies, one may consider the expansion

$$\sum_p \frac{|V_{pq}|^2}{E - \zeta_p^0} \approx \frac{A}{E - \langle \zeta \rangle} + \frac{B}{(E - \langle \zeta \rangle)^3} + \dots,$$

where $\langle \zeta \rangle$ is an appropriately weighted average of the ζ_p^0 's. Such an expansion is valid outside of R . Considering the first term only, the zeros would occur at

$$E \approx \frac{1}{2} [\epsilon_q^0 + \langle \zeta \rangle \pm \sqrt{(\epsilon_q^0 - \langle \zeta \rangle)^2 + 4A}] \\ \approx \frac{1}{2} \left[\epsilon_q^0 + \langle \zeta \rangle \pm |\epsilon_q^0 - \langle \zeta \rangle| \left(1 + \frac{2A}{|\epsilon_q^0 - \langle \zeta \rangle|^2} - \dots \right) \right],$$

provided that both energies lie outside of R . The first will lie below R , but the second may lie within R or above it. In the latter case, the high-energy pole betrays a state resulting from the strong level repulsion between $|q\rangle$ and a unique, coherent superposition of the $|p\rangle$'s. This is a bound state analogous to a two-hole, quasibound final states found in Auger spectroscopy of solids. In the former case, the above expansion must be abandoned, and one instead finds an enhancement in the density of states somewhere in R . As the pole approaches R from above, the density of states in R is enhanced on the high-energy side.

- ¹W. Kohn and L. J. Sham, Phys. Rev. **140**, 1133 (1965).
- ²M. S. Hybertsen and S. G. Louie, Phys. Rev. Lett. **55**, 1418 (1985); Phys. Rev. B **34**, 5390 (1986).
- ³J. E. Northrup, M. S. Hybertsen, and S. G. Louie, Phys. Rev. Lett. **59**, 819 (1987); Phys. Rev. B **39**, 8198 (1989); M. P. Surh, J. E. Northrup, and S. G. Louie, *ibid.* **38**, 5976 (1988).
- ⁴I use atomic units, where the energy unit is the Hartree energy (27.2114 eV), as well as the electron volt (eV).
- ⁵See L. Hedin and S. Lundqvist, in *Solid State Physics*, edited by H. Ehrenreich, F. Seitz, and D. Turnbull (Academic, New York, 1969), Vol. 23, p. 1. The index “1” denotes space, spin and time coordinates; a “+” superscript denotes adding a positive infinitesimal to time.
- ⁶See X. Blase, A. Rubio, S. G. Louie, and M. L. Cohen, Phys. Rev. B **51**, 6868 (1995), and references therein.
- ⁷G. Baym and L. P. Kadanoff, Phys. Rev. **124**, 287 (1961).
- ⁸E. W. Plummer, Phys. Scr. **T17**, 186 (1987), and references therein; B. S. Itchkawitz, In-Whan Lyo, and E. W. Plummer, Phys. Rev. B **41**, 8075 (1990).
- ⁹G. D. Mahan and B. E. Sernelius, Phys. Rev. Lett. **62**, 2718 (1989).
- ¹⁰C. Bowen, G. Sugiyama, and B. J. Alder, Phys. Rev. B **50**, 14 838 (1994).
- ¹¹D. M. Ceperley and B. J. Alder, Phys. Rev. Lett. **45**, 566 (1980), as parametrized by S. H. Vosko, L. Wilk, and M. Nusair, Can. J. Phys. **58**, 1200 (1980).
- ¹²This is derived in A. L. Fetter and J. D. Walecka, *Quantum Theory of Many-Particle Systems* (McGraw-Hill, New York, 1971), pp. 67–69.
- ¹³B. I. Lundqvist and V. Samathiyakanit, Phys. Kondens. Mater. **9**, 231 (1969).
- ¹⁴Uncertainties include statistical uncertainties, systematic uncertainties regarding how to include discrepancies (as ratios or difference), and uncertainties in Ref. 3.
- ¹⁵B. I. Lundqvist, Phys. Kondens. Mater. **6**, 193 (1967).
- ¹⁶B. I. Lundqvist, Phys. Kondens. Mater. **6**, 206 (1967).
- ¹⁷B. I. Lundqvist, Phys. Kondens. Mater. **7**, 117 (1968).
- ¹⁸L. Hedin, Phys. Scr. **21**, 477 (1980).
- ¹⁹B. Bergesen, F. W. Kus, and C. Blomberg, Can. J. Phys. **51**, 102 (1973); P. Minnhagen, J. Phys. C **8**, 3898 (1970).
- ²⁰R. Del Sole, L. Reining, and R. W. Godby, Phys. Rev. B **49**, 8024 (1994).
- ²¹P. A. Bobbert and W. van Haeringen, Phys. Rev. B **49**, 10 326 (1994).
- ²²For instance, see J. A. Carlisle *et al.*, Phys. Rev. Lett. **74**, 1234 (1995).
- ²³This is reviewed by S. Doniach and E. H. Sondheimer, *Green’s Functions for Solid State Physicists* (Benjamin/Cummings, Reading, MA, 1974), pp. 200–212.
- ²⁴G. D. Mahan (private communication).
- ²⁵F. Aryasetiawan and U. von Barth, Phys. Scr. **T45**, 270 (1992); F. Aryasetiawan, Phys. Rev. B **46**, 13 051 (1992).
- ²⁶F. Aryasetiawan and O. Gunnarsson, Phys. Rev. Lett. **74**, 3221 (1995).
- ²⁷L. Mitaš, Bull. Am. Phys. Soc. **41**, 253 (1996).